

RESEARCH PAPER

## Highly Efficient Adsorbent for Removal of Heavy Metal Ions Modified by a Novel Schiff Base Ligand

Mohsen Amrollahi<sup>1</sup>, Mohammad Taghi Ghaneian<sup>1</sup>, Masoumeh Tabatabaei<sup>2\*</sup>,  
Mohammad Hassan Ehrampoush<sup>1</sup>

<sup>1</sup> Department of Environmental Health Engineering, Shahid Sadoughi University of Medical Sciences, Yazd, Iran

<sup>2</sup> Department of chemistry, Yazd Branch, Islamic Azad University, Yazd, Iran

### ARTICLE INFO

#### Article History:

Received 16 June 2018

Accepted 12 September 2018

Published 01 October 2018

#### Keywords:

Adsorption Isotherm

Modified Alumina

Nanoparticles

Removal Of Cr(VI)

### ABSTRACT

An alumina-based nano adsorbent was prepared by modification of the external surface of  $\gamma$ -alumina ( $\gamma\text{-Al}_2\text{O}_3$ ) nanoparticles with functional groups of a new Schiff base 4-[(2-hydroxy-3-methoxy-benzylidene)-amino]-5-methyl-2,4-dihydro-[1,2,4]triazole-3-thione] "L". In order to the removal of Cr(VI) from aqueous solutions, we used the reaction of the sodium dodecyl sulfate coated nano-alumina with L solution for. This new modifying strategy significantly improve removal efficiency due to facilitate the accessibility of Cr ions to the activated sits. The surface morphology and chemistry of the adsorbent was characterized by SEM and FT-IR spectroscopy, respectively. Effect of most important parameters such as effect of pH value, contact time, adsorbent dosage, and initial Cr(VI) concentration on removal efficiency were investigated. In order to interpret the results Langmuir and Freundlich isotherm models were used. The results show that prepared absorbent significantly remove heavy metal ions from wastewater.

#### How to cite this article

Amrollahi M, Ghaneian MT, Tabatabaei M, Ehrampoush MH. Highly Efficient Adsorbent for Removal of Heavy Metal Ions Modified by a Novel Schiff Base Ligand. J Nanostruct, 2018; 8(4): 374-382. DOI: 10.22052/JNS.2018.04.007

### INTRODUCTION

Cadmium, lead, mercury, and chromium are often detected in industrial wastewaters originated from metal plating, mining activities, tanneries, petroleum refining, paint manufacture, pigment manufacture, pesticides, printing and photographic industries, etc.,. The concentration of these metals in wastewater may therefore rise to a level that can be hazardous to human health, animals, and the aquatic environment that why detecting and removal of heavy metal ions has received increasing attention [1-3]. The removal and recovery of heavy metal ions from industrial wastewater have been a significant concern in most industrial branches due to economic and environmental factors [4-6]. Hexavalent chromium, Cr(VI), has been regarded as a typical heavy metal pollutant generated from industries including electroplating, pigment manufacture, metal cleaning, leather tanning,

mining, chromate preparation, as a biocide etc [7]. Soluble Cr(VI) is highly toxic, pollutes the soil and water, and causes cancer, skin allergies, genetic defects [8-10] that why it is necessary to eliminate Cr(VI) from the environment. According to the US Environmental Protection Agency (EPA), maximum contaminant level of Cr(VI) is 0.05 mg L<sup>-1</sup> in water [11, 12]. Several techniques including precipitation [13, 14], ion exchange [15], adsorption [16, 17], membrane separation (dialysis/electrodialysis [18], electrolysis [19], reverse osmosis [20]) etc., have been developed to remove of Cr(VI). Among these methods adsorption is one of the most promising and widely used method for remove heavy metal ions because of its high efficiency, easy handling, economical effectiveness and availability of different adsorbents. Therefore, choosing an economical, effective and environmentally friendly Cr(VI) adsorbent is very important. Using

\*Corresponding Author Email: tabatabaei@iauyazd.ac.ir

low cost and inexpensive biosorbents such as agricultural wastes, clay materials, biomass, and seafood processing wastes may be a suitable alternative for removal of heavy ions [21, 22]. However, to improve their absorption capacity and enhance the separation rate, the design and exploration of novel adsorbents are still necessary. Nowadays the attention is focused on developing novel alternative adsorbents with high adsorptive capacity and low cost. In this regard, much attention has recently been paid to nanoparticles [23, 24]. Nanoparticles exhibit good adsorption efficiency especially due to the very high surface/volume rate and higher active sites for interaction with metal ions. Furthermore, adsorbents with specific functional groups have been developed to improve the adsorption capacity [25]. Alumina is a classical adsorbent with two main phase ( $\alpha$ -alumina and  $\gamma$ -alumina) which  $\gamma$ -alumina show higher activity than  $\alpha$ -alumina [26, 27].  $\gamma\text{-Al}_2\text{O}_3$  nanoparticles is a promising material as a solid-phase adsorbent because of its large specific surface area, high adsorption capacity, mechanical strength and low temperature modification [25, 28, 29]. Main challenge for using alumina is that some heavy-metal ions are poorly adsorbed on it. Chemical modification of the surface of  $\gamma\text{-Al}_2\text{O}_3$  nanoparticles with certain functional groups containing some donor atoms is one promising method to overcome this problem [30-34]. Herein, a new and novel Schiff base "4-[(2-Hydroxy-3-methoxy-benzylidene)-amino]-5-methyl-2-4dihydro-[1,2,4]triazole-3-thione", L, was introduced as modifier for modify SDS coated alumina nanoparticles for removing of Cr(VI).

## EXPERIMENTAL

### Chemicals

All purchased chemicals were used without further purification.  $\gamma\text{-Al}_2\text{O}_3$  nanostructure was purchased from Noavarjan Nano Chimia Pazho company. A 500 mg L<sup>-1</sup> stock solution of Cr(VI) was prepared by dissolving of 0.1414 g K<sub>2</sub>Cr<sub>2</sub>O<sub>7</sub> in 100 mL distilled water. Working standard solutions were obtained by appropriate dilution of the stock standard solution. The metal ion solutions were prepared from 1000 mg L<sup>-1</sup> stock solutions containing nitrate salts. pH adjustments were performed with 1N H<sub>3</sub>PO<sub>4</sub> and NaOH solutions.

### Characterization

IR spectra were recorded using IR Spectra

Shimadzu spectrometer 883 (KBr pellets, 4000-400 cm<sup>-1</sup>). A UV-Vis spectrophotometer (SP-3000, Japan) equipped with 1.0 cm path length quartz cells was used to obtain absorbance spectra and absorbance curves at fixed wavelength in a given time period. IR spectra were recorded using FT-IR Spectra Bruker Tensor 27 spectrometer (KBr pellets, 4000–400 cm<sup>-1</sup>). <sup>1</sup>H-NMR was recorded on a Brucker (AX-200) 300MH spectrometer using TMS as an external standard. Elemental analyses were performed using a Costech ECS 4010 CHNS analyzer. A digital pH-meter (MI151, US) equipped with a combined glass electrode was used for the pH measurements. A mechanical shaker type of (GFL 137; Innova, UK) was used for stirring the solutions.

### Synthesis of 4-[(2-hydroxy-3-methoxy-benzylidene)-amino]-5-methyl-2,4-dihydro-[1,2,4]triazole-3-thione]

4-amino-5-methyl-2H-1,2,4-triazole-3(4H)-thione was prepared according to the previous report [35]. 1.30 g (10 mmol) of 4-amino-5-methyl-2H-1,2,4-triazole-3(4H)-thione was dissolved in 20 mL ethanol then 1.52 g (10 mmol) 2-hydroxy-3-methoxybenzaldehyde was added to above solution. Finally, the resulting mixture was acidified with 4 drops of hydrochloric acid (37.5 %). The reaction mixture was refluxed for 8 h. The progress of the reaction was monitored by TLC. After completion of the reaction, the obtained solid was filtered and washed with ethanol. Chemical structure of ligand is shown in Fig. 1.

### Preparation of $\gamma\text{-Al}_2\text{O}_3$ modified with L

0.16 g of SDS was dissolved in 100 mL water. Then 2.0 g of alumina nanoparticles were dispersed in the previous solution. Diluted solution of HCl was used to set the PH at 2. Afterward 10 mL of solution including 0.6 g of L in 20 ml ethanol was added to alumina nanoparticles /SDS mixture.

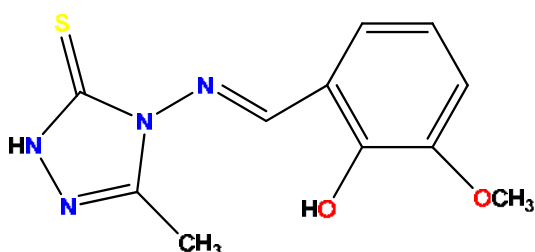


Fig. 1. Chemical structure of Schiff base

Finally the suspension was stirred at 50–60 °C to completely evaporate the solvent and modified residual was separated, washed and dried.

#### Remove Cr(VI)

In experimental batch,  $\gamma\text{-Al}_2\text{O}_3$ -SDS-L was added into Cr(VI) solution. After a certain period of time, 5 mL of the solution was taken out and measured the absorption at 540 nm using 1,5-diphenylcarbazide method [36]. The removal efficiency was determined by using the following equation:

$$R = \frac{(C_0 - C_e)}{C_0} \times 100 \quad (1)$$

Where  $C_0$  and  $C_e$  are the initial and final Cr(VI) concentrations in mg L<sup>-1</sup>, respectively. In order to improve the repeatability of the results, all the experiments repeated 3 time and the mean of the three measurements was reported. All the experiments were performed at 20 °C.

## RESULTS AND DISCUSSION

### Characterization of the adsorbent

Generally, the alumina surface is hydrophilic and has low adsorption affinity for organic compounds; however, when it is treated with sodium dodecyl sulfate (SDS), alumina will acquire high adsorption capability. When the pH of the solution is below the zero charge point of alumina (pH 8.5), the alumina surface is positively charged and anionic surfactants such as SDS molecules will adsorb onto the surface due to the electrostatic interaction [26]. In 1994, Hiraide et al. [30] proposed that water-insoluble organic ligand could be trapped into the surface of alumina particles capped sodium dodecyl sulfate (SDS). In the preliminary studies it was found that when schiff base "L" is mixed with SDS coated alumina particles, the ligand is attached to the SDS on alumina surface and shows similar

effect to that demonstrated for the other organic ligands [31–34]. That why the colour of alumina was changed from white to orange. In this work, the concentration of SDS was fixed at 5×10<sup>-3</sup> M, which is below the critical micelle concentration (CMC) of SDS (8×10<sup>-3</sup> M). In the concentration higher than the CMC, micelles would form in the aqueous solution and do not adsorbed on the alumina surface. Adsorbed SDS can trap molecules of schiff base "L" homogeneously, which causes the alumina to change color from white to orange (Fig. 2). Alumina nanoparticles capped SDS did not adsorb metal ions from the solution while L- $\gamma\text{-Al}_2\text{O}_3$  efficiently remove heavy metals from wastewater. That happens because absorbed Schiff Base on the surface of nanoparticles can form complex with metal ions.

The FT-IR of schiff base "L",  $\gamma$ -alumina and modified  $\gamma$ -alumina nanoparticles are shown in Fig. 3 (a, b, c). Comparison of the FT-IR spectrum of  $\gamma$ -alumina with a modified  $\gamma$ -alumina shows that many new peaks appeared in the FT-IR spectrum which approves present of L molecules on the surface of  $\gamma$ -alumina nanoparticles. A comparison between the FT-IR spectra in Fig. 3 indicated that the surface of L- $\gamma\text{-Al}_2\text{O}_3$  are contained –NH– functional group as a result of the immobilization procedure.

SEM analysis was used to study the effect of modifier on the morphology of final products. The results are shown in Fig. 4. As seen from the Figure, by using L ligand, products were aggregated.

There are several important parameters including PH, amount of absorbent, contacting time that effect on removal efficiency. In order to study the effect of PH, three different values 3, 5 and 7 were tested. For each experiment, 1 g/L of adsorbent was added onto 5 mg L<sup>-1</sup> solution of Cr(VI) at mentioned pH and then Cr(VI) remained values was measured. Fig. 5 presents the results

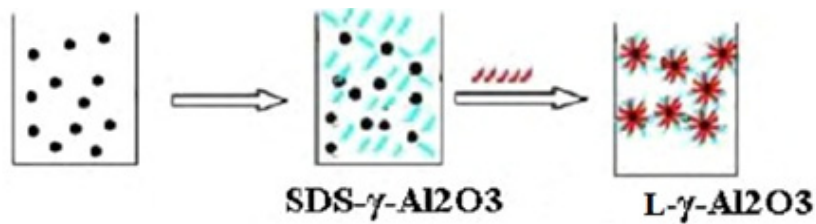


Fig. 2. Schematic of the functionalizing schiff base "L" on the alumina nanoparticles

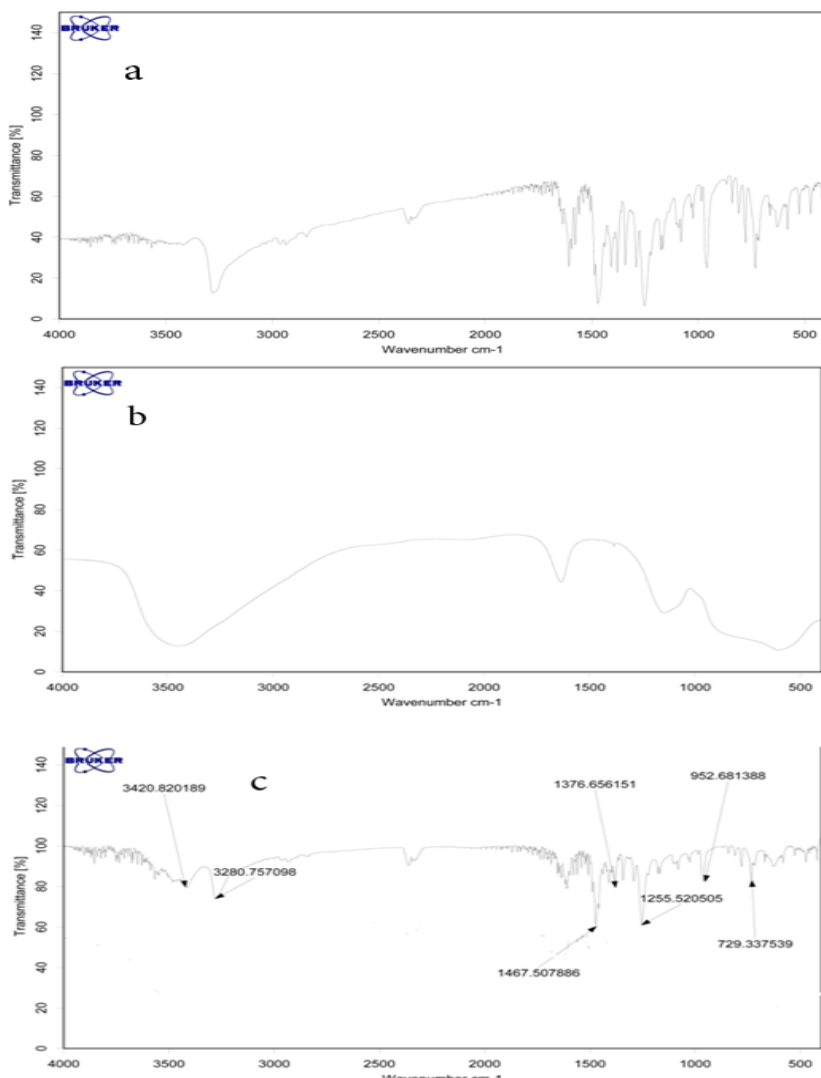


Fig. 3. a) FT-IR spectrum of schiff base "L", b) FTIR spectrum of alumina nanoparticles c) FTIR spectrum of modified alumina nanoparticles with L. FT-IR (KBr) ( ,  $\text{cm}^{-1}$ ): 3500-3100 (a), 1608 (s), 1581(s), 1388 (b), 1096 (s), 873 (m), 827 (m), 562(m), 445 (m). Anal.Calcd.for C<sub>11</sub>H<sub>12</sub>N<sub>4</sub>O<sub>2</sub>S: C, 49.94, H, 4.54, N, 21.19%. Found: C, 49.72, H, 4.43, N, 20.97%. 1H-NMR (Solvent DMSO), δ ppm: 2.33 (s, 3H, CH<sub>3</sub>), 3.84 (s, 3H, OCH<sub>3</sub>), 6.89-746 (3H, Ar and 1H, NH), 8.92 (s, 1H, CH=N), 13.50 (1H, OH).

for effect of the pH on the removal efficiency of Cr(VI) ions. It can be seen from Fig. 5 that the highest removal efficiency was 83.4% obtained at pH 3.0 while the lowest removal efficiency was 30% obtained at pH 7.0. All experiments were done on 20°C.

The effect of adsorbent quantity for removal efficiency was investigated by adding various amounts of adsorbent from 0.25 to 1.25 g/L into the beaker containing different concentration of Cr(VI) solutions (2, 5, 10 mg L<sup>-1</sup>) at pH = 3 for all batch experiments. However, the maximum removal efficiency of 97% was achieved after 24 h

under stirring condition (150 rpm) for 2 mg L<sup>-1</sup> of Cr(VI) and 1.25 g/L of adsorbent. The results are shown in Fig. 6.

Another important parameter that was investigated was stirring time. For this reason, adsorption processes carried out in different contact times including 15, 30, 60, 120 and 180 min. For each experiment, 0.1 g/100mL of adsorbent was added onto Cr(VI) solution with initial concentrations of 2, 5 and 10 mg L<sup>-1</sup> at pH 3.00 and then remained Cr(VI) was measured. We repeated each experiment several times and reported the average value. The standard deviation was less

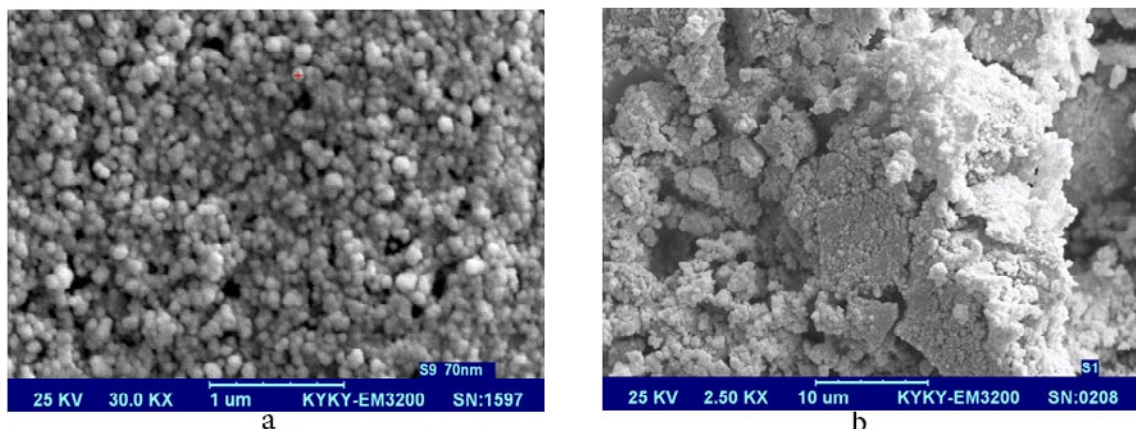


Fig. 4. The SEM image of  $\gamma$ - $\text{Al}_2\text{O}_3$  (a) and L- $\gamma$ - $\text{Al}_2\text{O}_3$  (b).

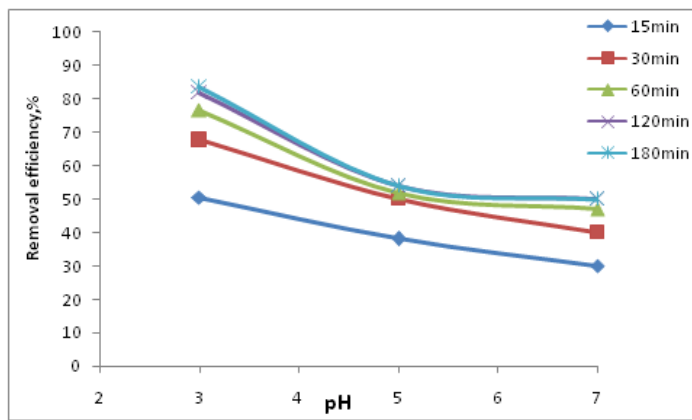


Fig. 5. The effect of pH on removal efficiency of Cr(VI) ions at different contact times.  
Conditions: 0.05 g/100ml of adsorbent mass, 5 mgL<sup>-1</sup> of Cr(VI) solution

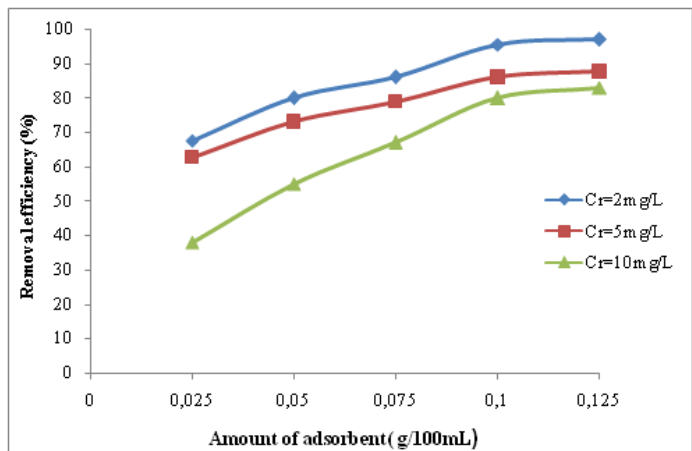


Fig. 6. Percentage removal of Cr(VI) at different amounts of adsorbent.

than 1.5%. The results were recorded and the time profile of Cr(VI) ions adsorption was plotted in the Fig. 7. According to the Fig.6, the optimum

contacting time for adsorption of the Cr(VI) ions was 180 min that leads to removal efficiency of 94.1%. All experiments were done on 20°C.

The correlation of equilibrium data by either theoretical or empirical models is essential to practical operation. Langmuir [37] and Freundlich [38] equations were used to analysis the experimental data of the  $\gamma\text{-Al}_2\text{O}_3\text{-SDS-L}$  adsorbents for Cr(VI). The absorption equilibrium curves for removal of Cr ions were evaluated by adding certain amount of  $\gamma\text{-Al}_2\text{O}_3\text{-SDS-L}$  in 50.0 mL solutions with different concentrations of Cr(VI) at pH 3.0. The amount of Cr(VI) in the solution were determined after equilibration. The general form of the Langmuir isotherm is:

$$\frac{q_e}{q_m} = \frac{K_L C_e}{1 + K_L C_e} \quad (2)$$

where  $K_L$  is a constant and  $C_e$  is the equilibrium concentration ( $\text{mg L}^{-1}$ ),  $q_e$  is the amount of Cr(VI) adsorbed per gram of adsorbent ( $\text{mg g}^{-1}$ ) at equilibrium concentration  $C_e$ , and  $q_m$  is the maximum amount of solute adsorbed per gram of surface ( $\text{mg g}^{-1}$ ), which depends on the number of adsorption sites. The Langmuir isotherm shows that the amount of adsorbed Cr(VI) increases by increasing the concentration up to a saturation point. First, adsorption will increase with increasing Cr(VI) concentrations, but as soon as all of the sites are occupied, a further increase in concentrations of Cr(VI) does not increase the amount of Cr(VI) on adsorbents (Fig. 8a). After linearization of the Langmuir isotherm, Eq. (2), we obtain:

$$\frac{C_e}{q_e} = \left( \frac{C_e}{q_m} \right) + \left( \frac{1}{K_L q_m} \right) \quad (3)$$

The Freundlich empirical model is represented by:

$$q_e = k_f C_e^{\frac{1}{n}} \quad (4)$$

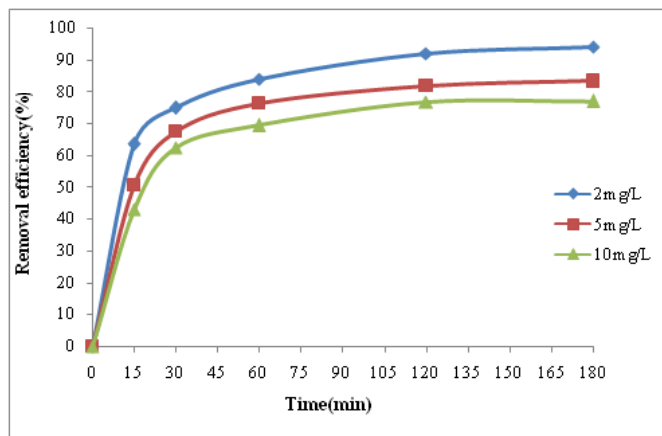


Fig. 7. Percentage removal of Cr(VI) at different times.

where  $K_f$  ( $\text{mmol}^{1-1/n} \text{L}^{1/n} \text{g}^{-1}$ ) and  $1/n$  are Freundlich constants that depend on the temperature and the given adsorbent–adsorbate couple,  $n$  is related to the adsorption energy distribution, and  $K_f$  indicates the adsorption capacity. The linearized form of the Freundlich adsorption isotherm equation is:

$$\ln q_e = \ln k_f + \left( \frac{1}{n} \right) \ln C_e \quad (5)$$

The Freundlich plot for Cr(VI) adsorption using the adsorbent is shown in Fig. 8b.

Using the appropriate constants for the Freundlich and Langmuir equations, the theoretical isotherm curves were predicted using known values of  $C_e$ . By comparison of the experimental points with the Freundlich and Langmuir isotherms, results show that both isotherms gave good agreement with the experimental data.

#### Adsorption kinetics

Kinetic models are used to examine the rate of the adsorption process and the potential rate controlling step. In the present work, the kinetic data obtained from batch studies have been analyzed using pseudo-first order and pseudo-second order models. For this purpose, 0.1 g/100ml of adsorbent was used, contact times were 15, 30, 60, 120, 180 minutes and the pH of the solutions was fixed at 3. The results are shown in Fig. 9(a, b). According to these Figure, the correlation coefficient values ( $R^2$ ) of pseudo-first order (Fig. 8a) and pseudo-second order models (Fig. 9b) were obtained 0.933 and 0.999, respectively. So, By comparison of those models, the correlation coefficients for the pseudo-

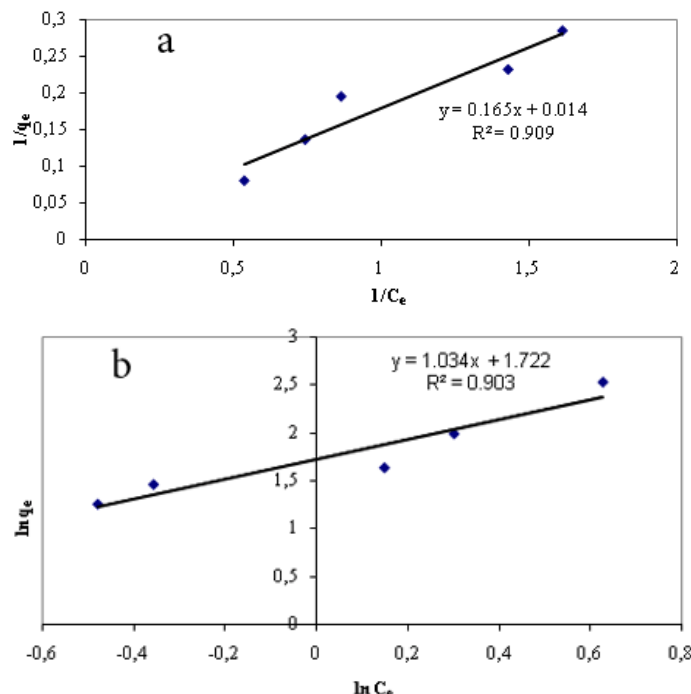


Fig. 8. a) Langmuir adsorption isotherm of Cr(VI) for modified  $\gamma$ -alumina nanoparticles. b) Freundlich adsorption isotherm of Cr(VI) for modified  $\gamma$ -alumina nanoparticles.

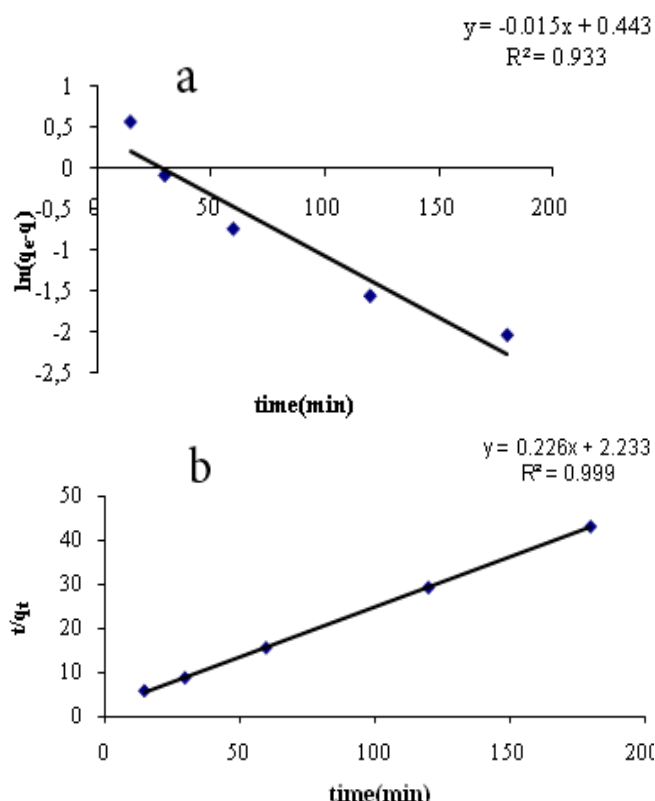


Fig. 9. a) Pseudo- first -order plot of kinetic adsorption curve of Cr(VI) on modified  $\gamma$ -alumina nanoparticles. b) Pseudo- second -order plot of kinetic adsorption curve of Cr(VI) on modified  $\gamma$ -alumina nanoparticles.

Table 1. Comparison of the proposed methods for the removal of Cr(IV) with some existing methods.

Type of adsorbent	Cr(VI) concentration (mg L <sup>-1</sup> )	Dose of adsorbent	Time (min)	adsorb %	Ref.
Acropitlon repense flower powder	2.0-10.0	0.5–2 g/L	180 min	55.6 –76.50	6
iron nanoparticles embedded in orange peel pith	10.0-50.0	2.5 g/L	60 min	25-71	39
algal bloom residue derived activated carbon	200	0.5–5 g/L	240 min	44.62-99.99	40
Ocimum americanum L. seed pods	100-200	8 g/L	120 min	100	41
alumina nanoparticles modified	2-10	0.25-1.25 g/L	180 min	68-94	Present study

second order kinetics model fits are higher than the correlation coefficients derived from pseudo-first order model fits. Given the good agreement between model fit and experimentally observed equilibrium adsorption capacity in addition to the large correlation coefficients, this suggests that the investigated Cr(VI) adsorption followed pseudo-second order kinetics and Cr(VI) ions were adsorbed onto the adsorbent surface via chemical interaction.

We compared our result with previous reports and results were tabled in Table 1. These Comparison clearly show that proposed absorbent show higher efficiency compare to the previous works.

## CONCLUSION

Herein, we report a novel adsorbent for removal of Cr ions. This is the first time that 4-[(2-hydroxy-3-methoxy-benzylidene)-amino]-5-methyl-2,4-dihydro-[1,2,4]triazole-3-thione] is used to modify alumina nanoparticles. These modified alumina nanoparticles efficiently remove Cr ions. Several important parameters that effect the removal efficiency such as PH, amount of adsorbent, contacting time were studied.

## CONFLICT OF INTEREST

The authors declare that there are no conflicts of interest regarding the publication of this manuscript.

## REFERENCES

- Zhang L, Zhai Y, Chang X, He Q, Huang X, Hu Z. Determination of trace metals in natural samples by ICP-OES after preconcentration on modified silica gel and on modified silica nanoparticles. *Microchimica Acta*. 2009;165(3-4):319-27.
- Soylak M, Tuzen M, Mendil D, Turkekul I. Biosorption of heavy metals on *Aspergillus fumigatus* immobilized Diaion HP-2MG resin for their atomic absorption spectrometric determinations. *Talanta*. 2006;70(5):1129-35.
- MikuÅ, B, Puzio B, Feist B. Application of 1,10-phenanthroline for preconcentration of selected heavy metals on silica gel. *Microchimica Acta*. 2009;166(3-4):337-41.
- Ngomzik A-F, Bee A, Siaugue J-M, Talbot D, Cabuil V, Cote G. Co(II) removal by magnetic alginate beads containing Cyanex 272®. *Journal of Hazardous Materials*. 2009;166(2-3):1043-9.
- Wang J, Chen C. Biosorbents for heavy metals removal and their future. *Biotechnology Advances*. 2009;27(2):195-226.
- Yin P, Xu Q, Qu R, Zhao G, Sun Y. Adsorption of transition metal ions from aqueous solutions onto a novel silica gel matrix inorganic-organic composite material. *Journal of Hazardous Materials*. 2010;173(1-3):710-6.
- Deng S, Bai R. Removal of trivalent and hexavalent chromium with aminated polyacrylonitrile fibers: performance and mechanisms. *Water Research*. 2004;38(9):2424-32.
- Zhao L, Sun J, Zhao Y, Xu L, Zhai M. Removal of hazardous metal ions from wastewater by radiation synthesized silica-graft-dimethylaminoethyl methacrylate adsorbent. *Chemical Engineering Journal*. 2011;170(1):162-9.
- Xu X, Gao B-Y, Tan X, Yue Q-Y, Zhong Q-Q, Li Q. Characteristics of amine-crosslinked wheat straw and its adsorption mechanisms for phosphate and chromium (VI) removal from aqueous solution. *Carbohydrate Polymers*. 2011;84(3):1054-60.
- Agarwal GS, Bhuptawat HK, Chaudhari S. Biosorption of aqueous chromium(VI) by *Tamarindus indica* seeds. *Bioresource Technology*. 2006;97(7):949-56.
- Park D, Yun Y-S, Kim JY, Park JM. How to study Cr(VI) biosorption: Use of fermentation waste for detoxifying Cr(VI) in aqueous solution. *Chemical Engineering Journal*. 2008;136(2-3):173-9.
- Daulton TL, Little BJ, Jones-Meehan J, Blom DA, Allard LF. Microbial reduction of chromium from the hexavalent to divalent state. *Geochimica et Cosmochimica Acta*. 2007;71(3):556-65.
- Thomson RC, Miller MK. Carbide precipitation in martensite during the early stages of tempering Cr- and Mo-containing low alloy steels. *Acta Materialia*. 1998;46(6):2203-13.
- Long C, Lu J, Li A, Hu D, Liu F, Zhang Q. Adsorption of naphthalene onto the carbon adsorbent from waste ion exchange resin: Equilibrium and kinetic characteristics. *Journal of Hazardous Materials*. 2008;150(3):656-61.
- Mohammadi T, Moheb A, Sadrzadeh M, Razmi A. Modeling of metal ion removal from wastewater by electrodialysis.

- Separation and Purification Technology. 2005;41(1):73-82.
16. Ghaneian MT, Ehrampoush MH, Arany AM, Jamshidi B, Dehvari M. Equilibrium and kinetic studies of Cr (VI) removal from synthetic wastewater by Acroptilon repense flower powder. Polish Journal of Chemical Technology. 2013;15(2):40-7.
  17. Seid-Mohammadi A, Sharifi Z, Shabanlo A, Asgari G. Simultaneous Removal of Turbidity and Humic Acid Using Electrocoagulation/Flotation Process in Aqua Solution. Avicenna Journal of Environmental Health Engineering. 2015;2(1).
  18. Pascal V, Laetitia D, Joël L, Marc S, Serge P. New concept to remove heavy metals from liquid waste based on electrochemical pH-switchable immobilized ligands. Applied Surface Science. 2007;253(6):3263-9.
  19. Dialynas E, Diamadopoulos E. Integration of a membrane bioreactor coupled with reverse osmosis for advanced treatment of municipal wastewater. Desalination. 2009;238(1-3):302-11.
  20. Liu F, Zhang G, Meng Q, Zhang H. Performance of Nanofiltration and Reverse Osmosis Membranes in Metal Effluent Treatment. Chinese Journal of Chemical Engineering. 2008;16(3):441-5.
  21. Munagapati VS, Yarramuthi V, Nadavala SK, Alla SR, Abburi K. Biosorption of Cu(II), Cd(II) and Pb(II) by Acacia leucocephala bark powder: Kinetics, equilibrium and thermodynamics. Chemical Engineering Journal. 2010;157(2-3):357-65.
  22. Qiu W, Zheng Y. Removal of lead, copper, nickel, cobalt, and zinc from water by a cancrinite-type zeolite synthesized from fly ash. Chemical Engineering Journal. 2009;145(3):483-8.
  23. Afkhami A, Saber-Tehrani M, Bagheri H. Modified maghemite nanoparticles as an efficient adsorbent for removing some cationic dyes from aqueous solution. Desalination. 2010;263(1-3):240-8.
  24. Afkhami A, Norooz-Asl R. Removal, preconcentration and determination of Mo(VI) from water and wastewater samples using maghemite nanoparticles. Colloids and Surfaces A: Physicochemical and Engineering Aspects. 2009;346(1-3):52-7.
  25. Türker AR AR. New Sorbents for Solid-Phase Extraction for Metal Enrichment. CLEAN - Soil, Air, Water. 2007;35(6):548-57.
  26. Li J, Shi Y, Cai Y, Mou S, Jiang G. Adsorption of di-ethyl-phthalate from aqueous solutions with surfactant-coated nano/microsized alumina. Chemical Engineering Journal. 2008;140(1-3):214-20.
  27. Hiraide M, Iwasawa J, Hiramatsu S, Kawaguchi H. Use of Surfactant Aggregates Formed on Alumina for the Preparation of Chelating Sorbents. Analytical Sciences. 1995;11(4):611-5.
  28. Zhang L, Huang T, Zhang M, Guo X, Yuan Z. Studies on the capability and behavior of adsorption of thallium on nano-Al<sub>2</sub>O<sub>3</sub>. Journal of Hazardous Materials. 2008;157(2-3):352-7.
  29. Sharma YC, Srivastava V, Upadhyay SN, Weng CH. Alumina Nanoparticles for the Removal of Ni(II) from Aqueous Solutions. Industrial & Engineering Chemistry Research. 2008;47(21):8095-100.
  30. Hiraide M, Sorouradin M-H, Kawaguchi H. Immobilization of Dithizone on Surfactant-Coated Alumina for Preconcentration of Metal Ions. Analytical Sciences. 1994;10(1):125-7.
  31. Panahi-Kalamuei M, Alizadeh S, Mousavi-Kamazani M, Salavati-Niasari M. Synthesis and characterization of CeO<sub>2</sub> nanoparticles via hydrothermal route. Journal of Industrial and Engineering Chemistry. 2015;21:1301-5.
  32. Panahi-Kalamuei M, Rajabpour P, Salavati-Niasari M, Zarghami Z, Mousavi-Kamazani M. Simple and rapid methods based microwave and sonochemistry for synthesizing of tellurium nanostructures using novel starting reagents for solar cells. Journal of Materials Science: Materials in Electronics. 2015;26(6):3691-9.
  33. Panahi-Kalamuei M, Salavati-Niasari M, Zarghami Z, Mousavi-Kamazani M, Taqriri H, Mohsenikia A. Synthesis and characterization of Se nanostructures via co-precipitation, hydrothermal, microwave and sonochemical routes using novel starting reagents for solar cells. Journal of Materials Science: Materials in Electronics. 2015;26(5):2851-60.
  34. Shabani AMH, Dadfarnia S, Dehghani Z. On-line solid phase extraction system using 1,10-phenanthroline immobilized on surfactant coated alumina for the flame atomic absorption spectrometric determination of copper and cadmium. Talanta. 2009;79(4):1066-70.
  35. Justus Liebigs Ann Chem. 1960;637(1).
  36. Salavati-Niasari M, Mahmoudi T, Amiri O. Easy Synthesis of Magnetite Nanocrystals via Coprecipitation Method. Journal of Cluster Science. 2012;23(2):597-602.
  37. Langmuir I. THE ADSORPTION OF GASES ON PLANE SURFACES OF GLASS, MICA AND PLATINUM. Journal of the American Chemical Society. 1918;40(9):1361-403.
  38. Freundlich H, Heller W. The Adsorption of cis- and trans-Azobenzene. Journal of the American Chemical Society. 1939;61(8):2228-30.
  39. Salavati-Niasari M, Behfard Z, Amiri O, Khosravifard E, Hosseinpour-Mashkani SM. Hydrothermal Synthesis of Bismuth Sulfide (Bi<sub>2</sub>S<sub>3</sub>) Nanorods: Bismuth(III) Monosalicylate Precursor in the Presence of Thioglycolic Acid. Journal of Cluster Science. 2013;24(1):349-63.
  40. Amiri O, Hosseinpour-Mashkani SM, Mohammadi Rad M, Abdvali F. Sonochemical synthesis and characterization of CdS/ZnS core-shell nanoparticles and application in removal of heavy metals from aqueous solution. Superlattices and Microstructures. 2014;66:67-75.
  41. Levankumar L, Muthukumaran V, Gobinath MB. Batch adsorption and kinetics of chromium (VI) removal from aqueous solutions by Ocimum americanum L. seed pods. Journal of Hazardous Materials. 2009;161(2-3):709-13.

